ISSN 0097-8078, Water Resources, 2023, Vol. 50, No. 5, pp. 748–758. © Pleiades Publishing, Ltd., 2023.
Russian Text © The Author(s), 2023, published in Vodnye Resursy, 2023, Vol. 50, No. 5, pp. 602–612.

STUDIES OF THE PROCESSES OF INTERACTION BETWEEN LAND AND THE ATMOSPHERE AND THE HYDROLOGICAL EFFECTS OF CLIMATE CHANGE

Roughness Parameter of Shallow Water Bodies

I. A. Repina[a, b, c, *], A. Yu. Artamonov[a], I. A. Kapustin[d], A. A. Mol'kov[d], and V. M. Stepanenko[a, b, c, e]

[a] *Obukhov Institute of Atmospheric Physics, Russian Academy of Sciences, Moscow, 119017 Russia*
[b] *Research Computing Center, Moscow State University, Moscow, 119234 Russia*
[c] *Moscow Center of Fundamental and Applied Mathematics, Moscow, 119991 Russia*
[d] *Institute of Applied Physics, Russian Academy of Sciences, Nizhny Novgorod, 603950 Russia*
[e] *Water Problems Institute, Russian Academy of Sciences, Moscow, 119333 Russia*
**e-mail: repina@ifaran.ru*

Received February 6, 2023; revised February 6, 2023; accepted March 20, 2023

Abstract—The results of measurements of atmospheric turbulence characteristics were used to obtain parameterizations for calculating the dynamic roughness parameter and the roughness parameters for temperature and humidity for a shallow closed water body. At medium wind speeds, the results of calculations by Charnock formula are in agreement with observation data; in this case, the c parameter is three times as large as that in the case of an open ocean, and the passage from the viscous to wave mechanism occurs at high wind speeds, while the dynamic roughness parameter at the same wind speeds is greater. The roughness parameters for temperature and humidity at wind speed from 0.5 to 3 m/s are not equal. The empirical coefficients in the equations describing the ratio of the dynamic roughness to the roughness parameter for temperature (humidity) on Reynolds number are close to those obtained before for other closed water bodies, thus suggesting a common formation mechanism of transport processes in a viscous sublayer. The obtained parameterizations can be used in Earth system models and lake models for calculating turbulent flows over continental water bodies.

Keywords: closed water bodies, wind waves, dynamic roughness parameter, roughness parameter for temperature and humidity, Charnock parameter

DOI: 10.1134/S0097807823700045

INTRODUCTION

Exchange processes at the water–air interface are the key factor of hydrodynamic and environmental processes in aquatic ecosystems, the formation of weather and climate, the origination of currents, surface waves, and turbulent mixing, which has a direct effect on the transport of solutes [51], the characteristics of stratification [64], the oxygen regime and gas exchange [38]. The main characteristics of the interaction are vertical turbulent fluxes of momentum, heat, and moisture (sensible and latent heat). The knowledge of the magnitudes of these fluxes is necessary for numerical weather forecasts, simulation of the Earth system, interpretation of remote sensing data, and other geophysical applications.

The lack of knowledge on the structure of the surface layer of the atmosphere and its exchange of momentum, heat, and moisture with a rough water surface under different background conditions is now the main obstacle for the correct functioning of operational, global, and regional weather forecast models and expert models of climate change.

The transport of momentum between the atmosphere and water surface is largely determined by the roughness characteristics of momentum, temperature, and humidity. In addition, the momentum flux is affected by wind speed; atmospheric stratification; and the size, steepness, and phase velocity of wind waves and swell. The issue of the properties of the surface roughness parameters of shallow water areas is still largely open, despite numerous studies. This is especially true for small water areas, where wind wave parameters do not depend on the fetch and are determined by wind direction and topography characteristics.

In the numerical simulation of the boundary layer, the averaged fluxes are calculated with the use of the so-called aerodynamic bulk formulas [24]:

$$\tau = \rho C_D U_z^2, \quad (1)$$

$$H = \rho c_p C_H U_z (T_s - T_z), \quad (2)$$

$$LH = L_s \rho C_E U_z (q_s - q_z), \quad (3)$$

where C_D, C_H, C_E are dimensionless exchange coefficients (the resistance factor, Stanton number, and Dalton number, respectively); c_p and ρ are air heat capacity and density, L_s is boiling heat; τ, H, and LH are turbulent fluxes of momentum, heat, and moisture, respectively; U_z, T_z, and q_z are wind speed and air temperature and humidity at elevation z, respectively; T_s and q_s are the temperature and humidity at the surface. The exchange coefficients commonly refer to a standard elevation of measurements $z = 10$ m and to neutral stratification conditions.

This method enables the use of data of standard meteorological measurements; however, the main problem is the evaluation of exchange coefficients.

The equations of the Monin–Obukhov similarity theory (MOST) [4] yield the expressions:

$$C_D = \frac{\kappa}{\left[\ln\dfrac{z}{z_{0u}} - \Psi_m\left(\dfrac{z}{L}\right) + \Psi_m\left(\dfrac{z_{0u}}{L}\right)\right]}, \quad (4)$$

$$C_H = \alpha_T C_D \frac{[\ln z/z_{ou} - \Psi_u(z/L) + \Psi_u(z_{0u}/L)]}{[\ln z/z_{oT} - \Psi_T(z/L) + \Psi_T(z_{0T}/L)]}, \quad (5)$$

$$C_E = \alpha_q C_D \frac{[\ln z/z_{ou} - \Psi_u(z/L) + \Psi_u(z_{0u}/L)]}{[\ln z/z_{oq} - \Psi_T(z/L) + \Psi_q(z_{0q}/L)]}, \quad (6)$$

where $\alpha_T = K_T/K_m$ and $\alpha_q = K_q/K_m$ are the ratios of turbulent thermal conductivity and diffusion coefficients to viscosity, or inverse turbulent Prandtl and Schmidt numbers, respectively; z is measurement height; z_{0u} is the parameter of dynamic (or aerodynamic) roughness; z_{0T} and z_{0q} are the roughness parameters for temperature and specific humidity, i.e., elevations at which the wind speed, temperature, and humidity reach surface values, if the profile of appropriate meteorological characteristics is extrapolated to the surface. The integral universal functions Ψ_a are defined as follows: $\Psi_a = \int_0^{\zeta} \frac{1-\phi_a(\zeta)}{\zeta} d\zeta$, $\phi_a(\zeta)$ are universal functions, describing the profiles of meteorological characteristics, $\zeta = \frac{z}{L}$ is a dimensionless stability parameter, $L = \frac{u_*^3}{\kappa\left(\frac{g}{T_0}\right)\left(\frac{H}{c_p\rho}\right)}$ is Obukhov's scale.

The parameterizations for determining the universal functions have been developed based on numerous special experiments under different stratification conditions [16, 23, 32, 53] and adequately describe the profiles of meteorological characteristics under the conditions of stationarity and homogeneous relief. The roughness characteristics z_{0u}, z_{0T}, and z_{0q} are physical variables not measured directly. They are introduced into similarity formulas in order to avoid detailed description of wind speed and temperature profiles in the immediate vicinity to the underlying surface, i.e., in the viscous sublayer. In MOST, the roughness parameters determine the interaction between the viscous sublayer, in which momentum and scalar variables are transferred by molecular heat conductance, diffusion, and viscosity, and the rough surface [14, 30]. In the viscous sublayer, the transport of momentum through the surface is mainly due to the pressure difference on opposite faces of the roughness elements, and the heat transfer is due to molecular thermal conductivity. This contrast leads to a difference between the roughness scales for wind speed z_{0u} (dynamic roughness) and for scalars (in particular, temperature and humidity) [79]. The parameter of dynamic roughness for different land surfaces in a developed turbulent flow is primarily determined by the sizes and shapes of roughness elements [14, 30] (except for the cases where the height of roughness elements is comparable with the Obukhov length scale, for example, in the case of urban development [80]), i.e., it can be evaluated based on the structure of the surface. The roughness parameters for the temperature and humidity are more variable and depend on a larger number of factors, including molecular viscosity and heat conductance [6, 66].

In the case of sea surface, the evaluation of dynamic roughness parameter is complicated by the dependence of the state of the surface on wind speed. Notwithstanding the numerous works in this field, there is still no clear understanding of the character of the dependence of the dynamic roughness parameter and the resistance of the water surface, associated with it, on the mean wind speed, wave character and age, and the dynamic and temperature state of the sea surface. The roughness of water surface is due to the motion of the air layer in contact with it and is maintained mostly by the transfer of momentum and energy to the surface. The small-scale roughness of the sea surface is a complex combination of gravity waves and capillary ripples, the origin and structure of which depend not only on the wind, but also on currents, internal waves in the sea and atmosphere, water body depth, bed topography, the effect of moving and stationary objects, anthropogenic surface pollution, and other factors [21, 25].

In terms of the impact of water bodies on the climate system, of particular interest are inland water bodies, i.e., lakes and reservoirs [19, 56]. The surface of lakes differs from the surrounding landscape by a small albedo, much lesser roughness, high thermal conductance, and high heat capacity; therefore, they have an effect on the processes in the atmospheric boundary layer, local atmospheric circulation, and the heat and water balance at regional scale [31, 46], which should be taken into account in the regional and climatic simulation.

However, in the majority of lake models, the schemes of parameterization of exchange processes are still based on oceanic data [33, 47, 68, 79]. Because of the difference between wave formation processes in an ocean and a lake, associated with the depth of the water body and the limited wave run, this approach can lead to significant errors [62]. Thus, it was found that lake surface can be aerodynamically rougher than the open ocean, the wind speed being the same; the use of oceanic parameterizations may lead to an error in the annual estimate of evaporation over the lake by 40% [44]. Therefore, attention should be paid to the parameterization of the exchange coefficients and roughness characteristics for lake models. Studies in this direction have been carried out before [13, 34, 35, 52, 67], but the issue of the properties of the roughness parameter for the surface of shallow water areas, in particular, lakes, is still largely open.

The main criterion for determining wind waves in shallow areas is $H \le \lambda/2$ (H is water body depth, and λ is the characteristic wave length) [2]. For the conditions of deep water, the largest resistance to the wind is due to the high-frequency components of the spectrum of sea waves; because their phase velocities are much less than the phase velocities in the vicinity of the spectral maximum of waves ω_0, and hence, the air flow velocity. The long and gently sloping waves, corresponding to the maximum of the spectrum of sea waves and having phase velocities close to the wind speed, do not produce appreciable tangential resistance to air flow, but can introduce wave resistance. The waves in shallow areas have relatively low phase velocities because of the limiting effect of water depth at a relatively high steepness, which is due to the nonlinear interaction between long and short waves. Because of this, the contribution of the components of wave spectrum to the total resistance of water surface near the maximum of the spectrum with a frequency ω_0 is comparable with the contribution of the high-frequency components and even predominant. This effect increases with a decrease in water body depth, i.e., the parameter of dynamic roughness increases with increasing wind speed or decreasing depth. In addition, asynchronous interaction between changes in surface wave characteristics and wind speed field takes place in small lakes. An important distinction of wave formation in lakes compared with that in the ocean is the short fetch. As the result, the wave field is characterized by young and high-frequency waves, and the measured values of wave age exceed the literature data. Therefore, the estimates obtained in the open ocean and even in shallow coastal zone are inapplicable to the parameterization of exchange processes in inland water bodies.

A fact that is also not taken into account is that the conditions of gentle winds are more typical of inland water bodies than of an open ocean [77], and in this case, the roughness characteristics show effects of the heterogeneity of the surface tension and small-scale capillary waves [48, 75].

Taking into account that the sensitivity of the determination of turbulent fluxes and the atmosphere–water surface interface to the choice of the scheme for determining roughness parameters is high [74], it is necessary to develop reliable schemes for calculating these parameters, in particular, in the case of shallow water bodies.

METHODS FOR DETERMINING THE ROUGHNESS PARAMETER

According to MOST, the roughness parameters z_{0u}, z_{0T}, and z_{0q} are determined as elevations at which the profiles of the appropriate weather characteristics are zero.

$$u = \frac{u_*}{\kappa}\left[\ln\left(\frac{z}{z_{0u}}\right) - \Psi_u\left(\frac{z}{L}\right) + \Psi_u\left(\frac{z_{0u}}{L}\right)\right]. \qquad (7)$$

For the temperature (and in a similar way, for humidity)

$$T = T_s + \frac{T_*}{\kappa_T}\left[\ln\left(\frac{z}{z_{0T}}\right) - \Psi_T\left(\frac{z}{L}\right) + \Psi_T\left(\frac{z_{0T}}{L}\right)\right], \qquad (8)$$

$T_* = \dfrac{H}{u_*}$, T_s is the temperature of the surface or the aerodynamic temperature (air temperature at roughness height).

Formulas (4)–(6) and (7), (8), yield the following relationships for the roughness parameters

$$z_{0u} = z\exp\left\{-\left[\frac{\kappa}{\sqrt{C_D}} + \Psi_m\left(\frac{z}{L}\right) - \Psi_m\left(\frac{z_0}{L}\right)\right]\right\}, \qquad (9)$$

$$z_{0T} = z\exp\left\{-\left[\frac{\kappa\sqrt{C_D}}{C_H} + \Psi_h\left(\frac{z}{L}\right) - \Psi_h\left(\frac{z_0}{L}\right)\right]\right\}, \qquad (10)$$

$$z_{0q} = z\exp\left\{-\left[\frac{\kappa\sqrt{C_D}}{C_E} + \Psi_h\left(\frac{z}{L}\right) - \Psi_h\left(\frac{z_0}{L}\right)\right]\right\}. \qquad (11)$$

In this study, universal functions are used in the following form [16, 23, 27, 32, 36]:

unstable stratification $\zeta < -0.05$:

$$\Psi_u = \frac{\Psi_{\text{kanzas}} + \zeta^2\Psi_{\text{conv}}}{1+\zeta^2}, \qquad (12)$$

$$\Psi_{\text{kanzas}} = 2\ln\left(\frac{1+x}{2}\right) + \ln\left(\frac{1+x^2}{2}\right) - 2\arctan x + \frac{\pi}{2}, \qquad (13)$$

$$\Psi_{\text{conv}} = \frac{3}{2}\ln\left(\frac{y^2+y+1}{3}\right) - \sqrt{3}\arctan\frac{2y+1}{\sqrt{3}} + \frac{\pi}{\sqrt{3}}, \qquad (14)$$

$$x = (1-19.3\zeta)^{1/4}, \quad y = (1-13\zeta)^{1/3},$$

$$\Psi_T(\zeta) = 2\ln\left(\frac{1+x^2}{2}\right), \quad x = 0.95(1-11.6\zeta)^{1/2}; \qquad (15)$$

neutral stratification: $-0.05 < \zeta < 0.05$:

$$\Psi_u(\zeta) = 0, \quad C_{Dn} = C_D; \tag{16}$$

stable stratification $\zeta > 0.05$:

$$\Psi_u(\zeta) = -6\zeta, \quad \Psi_T(\zeta) = -7.8\zeta. \tag{17}$$

The determination of the coefficients of exchange and Obukhov scale (stability parameter) by this method requires direct pulsation measurements of atmospheric turbulence characteristics. Despite the fact that the calculation uses empirical universal functions, this method is the only direct way to determine the roughness parameter.

When profile measurements are available, the dynamic roughness parameter can be calculated with the use of a formula for determining logarithmic wind profile under neutral stratification $u = \frac{u_*}{\kappa}\left[\ln\left(\frac{z}{z_{0u}}\right)\right]$. In this case, z_{0u} can be readily determined by measurements at two levels

$$\ln z_{0u} = \frac{\ln z_2 - \frac{u_2}{u_1}\ln z_1}{1 - \frac{u_2}{u_1}}, \tag{18}$$

z_1 and z_2 are the upper and lower levels at which wind speeds u_1 and u_2 are measured.

Taking into account that, at the interaction between the atmosphere and the rough surface, there exists a displacement height D, to which the atmospheric flow shifts in the vertical direction [80], the formulas for the logarithmic profile of wind and (18) are to be rewritten as

$$\frac{U_z}{u_*} = \kappa^{-2}\ln\left(\frac{z - D}{z_{0u}}\right), \tag{19}$$

$$z_{0u} = (z - D)\exp\left(\frac{-\kappa U_z}{u_*}\right) = (z_2 - z_1)\Big/\left[\exp\left(\frac{-\kappa u_2}{u_*}\right) - \left(\frac{-\kappa u_1}{u_*}\right)\right], \tag{20}$$

$$D = z_1 - \frac{z_2 - z_1}{\exp\left(\frac{-\kappa(u_2 - u_1)}{u_*}\right) - 1}.$$

Formula (20) requires additional data on the dynamic velocity. However, the displacement depth D of the water surface is insignificant, especially, in the case of weak and moderate winds, therefore, it can be ignored.

The calculation of the roughness parameter from (18) under real conditions can lead to errors because of the deviation of the actual wind speed profile from the logarithmic law at atmospheric stratification other than neutral. The application of the profile method is justified if the measurement levels of meteorological parameters are not high; it is applicable only for fixed basements and requires wind speed measurements by the same type of sensors with a high accuracy. The values of z_{0u} thus obtained from the logarithmic profile, constructed by data of $u(z)$ at two levels, differ only slightly even in the cases of highly stable and highly unstable stratification, if the measurements are made at levels of up to ~5 m above the surface [42]. Corrections for stratification due to the functions $\Psi_u(\zeta)$ and $\Psi_T(\zeta)$ are also small at strong winds, when $L \to \pm\infty$ and $\Psi_u(\zeta), \Psi_T(\zeta) \to 0$.

In the recent decades, various schemes were developed for the evaluation of the roughness parameter of water surfaces [25, 45, 57, 68], some of which take into account the stratification of the atmosphere [79].

The parameterization of the roughness conditions at the water–air interface in the model of interaction between the atmosphere and the ocean is commonly made with the use of Charnock formula [18]:

$$z_{0u} = a\frac{u_*^2}{g}, \tag{21}$$

where a is an empirical coefficient referred to as Charnock parameter. Experimental data [12] show that the values of Charnock coefficient can vary within more than an order of magnitude, depending on the conditions, and depend significantly on the characteristics of surface waves and water body depth. Various attempts were made to relate the roughness parameter with the parameters of sea waves. Based on numerous laboratory and field experiments and theoretical calculations, the parameter characterizing the roughness of the sea surface was taken to be the age of waves, defined as $\left(\frac{c_{ph}}{u_*}\right)$ or $\left(\frac{c_{ph}}{u_z}\right)$, where c_{ph} is wave phase velocity. Additional parameters are the frequency of the spectral peak of wind waves [63] and wave height.

Some researchers [22, 26, 39, 40, 49, 58] proposed a generalized formula to describe the dependence of the roughness coefficient on the wave age parameter in the form

$$\frac{g z_{0u}}{u_*^2} = f\left(\frac{c_{ph}}{u_*}\right). \tag{22}$$

For the limiting development of waves in shallow water bodies, when the surface roughness characteristics cease to depend on the fetch, as well as in the case of the transformation of waves coming from the open sea (large fetches), the following equation is used [5]

$$\frac{g z_{0u}}{u_*^2} = f\left(\frac{g h}{u_*^2}\right), \tag{23}$$

where h is water body depth. Based on dimensional considerations, the dependence (23) can be approximated by the formula

$$z_{0m} = m\frac{u_*^4}{g^2h}. \quad (24)$$

The value of the coefficient m is chosen using the conditions that in the case of developed waves and deep sea, Charnock parameter $a = \frac{gz_{0u}}{u_*^2} \to 0.011$; it varies from 25 to 50, depending on the depth of the water body and the distance from the shore. The measurement data show that this approach is applicable to coastal zones, but in some cases, it cannot be used for closed inland water bodies.

In the case of an oceanic surface, as Charnock supposed in his theoretical studies, the parameter a has an order of magnitude of 10^{-2} ([17, 18], $a = 0.0123$). This was confirmed by later studies (in [57], $a = 0.011$). According to [7], the values of Charnock parameter for shallow water bodies can differ considerably from those for the ocean. For example, higher values of a were found in studies [29] ($a = 0.0144$), [76] ($a = 0.018$), and [55] (greater by an order of magnitude: $a = 0.110$). For lakes and coastal zones, some researchers substantiate the value $a = 0.03$ [12, 29, 59, 70].

Under light winds, the water surface can be regarded as a smooth solid wall, separated from the near-wall flow by a viscous sublayer. The predominance of the viscous mechanism of roughness parameter formation of sea surface is observed at wind speed <5 m/s. Therefore, in the schemes of aerodynamic roughness parameterization, two situations are commonly considered: a current associated with wind stress [18, 57] and a current associated with viscosity.

With viscosity taken into account, the Charnock formula can be rewritten as

$$z_{ou} = c\frac{\nu}{u_*} + a\frac{u_*^2}{g}, \quad (25)$$

where ν is air kinematic viscosity (m^2/s), which is equal to $\sim 1.5 \times 10^{-5}$ m^2/s for the atmosphere at sea level. The parameter c is related to the Reynolds number Re, and, under oceanic conditions, it is taken equal to 0.11; in the case of lakes it can increase to 0.54 [72].

The roughness parameters for temperature and humidity are evaluated with the use of an approach first proposed by S.S. Zilitinkevich [1], where its dependence on Re and the parameter of dynamic roughness is parameterized. In the general form, this relationship can be written as

$$\ln\frac{z_{0u}}{z_{0T,q}} = a\,\mathrm{Re}^n + b, \quad \mathrm{Re} = \frac{z_{0u}u_*}{\nu}. \quad (26)$$

The coefficients a and b depend on the type of the surface and are determined from measurement data; the exponent n corresponds to various simplifications in equations of transport–diffusion of a scalar variable (temperature, humidity) in a viscous sublayer [43]. In different parameterizations, the values $n = 1$; 0.5; 0.25 are used [66]. Formula (26) can be rewritten as [62]:

$$\ln\frac{z_{0u}}{z_{0T}} = \frac{\kappa}{\mathrm{Pr}}(a\,\mathrm{Re}^n + b), \quad \ln\frac{z_{0u}}{z_{0q}} = \frac{\kappa}{\mathrm{Sc}}(a\,\mathrm{Re}^n + b), \quad (27)$$

where κ is Karman's constant, Pr = 0.71 is molecular Prandtl number for air, Sc = 0.66 is molecular Schmidt number of water vapor.

Reviews of roughness parameterizations for various surfaces can be found in [6, 14]. In the case of sea surface, the parameterization proposed in S.S. Zilintkevich study [79] is used. For the case of lakes, roughness parameterizations were tested in [20, 59, 62, 67, 71]. However, lake models, as before, are mostly based on the parameterizations developed for the open sea.

DATA AND PROCESSING METHODS USED

The parameterizations of the roughness parameters are analyzed using data of measurements of atmospheric turbulence characteristics in Bol'shoi Vilyui Lake [61] and the Mozhaisk and Gorky reservoirs. The average depth of Bol'shoi Vilyui Lake is 4 m, and that of the Mozhaisk and Gorky reservoirs is 20 m. On the lake and the Mozhaisk Reservoir, the measurement complex was located at a distance from the shores on an anchored floating base. In the Gorky Reservoir, *Geofizik* catamaran was used for measurements [3]. During the measurements, the direction of wind ensured a sufficient length of wave fetch, thus allowing the effect of shore to be neglected. The roughness parameters were determined by formulas (9)–(11), where the values of the coefficients of exchange, dynamic velocity u_*, heat and moisture fluxes, and the stability parameter $\zeta = \frac{z}{L}$ where used. In formulas (24) and (25), the values of u_* where also taken from measurements. The measurements were carried out on the Bol'shoi Vilyui in the summer of 2015; on the Mozhaisk Reservoir, in 2017; and on the Gorky Reservoir, in 2016–2018.

The measurement system consisted of an acoustic anemometer (WindMaster 3D brand, manufactured by Gill Instruments) and an open infrared CO_2/H_2O gas analyzer (LI 7500 brand, manufactured by LI-COR, Inc.). The gas analyzer was not used in Bol'shoi Vilyui Lake, where only the dynamic roughness parameter and the roughness parameter for temperature were determined. The data of acoustic anemometer were synchronized with gas analyzer data and used to calculate turbulent heat, momentum, and methane fluxes. The fluxes were calculated with the use of turbulent pulsation method (Eddy-covariance) [15].

In this method, the fluxes are calculated by covariations between the measured pulsations of meteorological parameters and gas concentrations:

$$\tau = \rho_0 u_*^2 = -\rho_0 \left[\mathbf{i}\overline{u'w'} + \mathbf{j}\overline{v'w'} \right], \quad (28)$$

$$H = c_p \rho_0 \overline{w'T'}, \quad (29)$$

$$LH = L_s \rho C_E \overline{w'q'}. \quad (30)$$

The denotations correspond to those in (1)–(3); u', v', w' are pulsations of the three components of wind velocity: longitudinal, transverse, and vertical, respectively; T' is temperature pulsation; q' is humidity pulsation. The calculation of fluxes was made with the use of spectral correction [50], density fluctuation correction [73], acoustic temperature correction [65], anemometer slope correction, as well as statistical tests [69]. Data quality control was carried out with the use of methods proposed in [28]. The footprint (the zone of flow formation on the surface) was evaluated using an analytical model [41]. The averaging period was taken equal to 20 min.

However, even at all corrections, the data on turbulent fluxes commonly have a large random spread. Accordingly, the roughness parameters evaluated by formulas (9)–(11) also show a wide spread. The only way to cope with this spread is to use additional corrections [9–11, 78]. The selection of data was carried out with the use of limitations on wind speed $u_* > 0.05$ m/s and on the values of fluxes $|H, LH| \geq 10$ W/m^2. Only the data corresponding to the domain of flow formation over water surface were used. During additional verification, the data were rejected if they met the following criteria [44]:

$$z_{0u}, z_{0T}, z_{0q} \geq 0.3 \text{ m}, \quad (31)$$

$$z_{0u} \leq 10^{-8} \text{ m}, \quad (32)$$

$$z_{0T}, z_{0q} \leq 10^{-7} \text{ m}. \quad (33)$$

The criterion (31) was applied in accordance with the assumption that the roughness scale does not exceed one tenth of the observation point elevation (maximum 3.0 m in this study). The criteria (32), (33) were used taking into account the transport of heat and moisture in the viscous sublayer [60]. It is supposed that at scales less than this level, the surface exchange of heat and moisture cannot take place [8, 11].

As the result of filtrations, 645 values of dynamic roughness parameter, 572 values of roughness parameter for the temperature, and 489 values for humidity were selected for the analysis.

MEASUREMENT RESULTS

Figure 1 shows the Charnock parameter obtained from the measurements (formulas (9), (21)). In the case of wind speed >5 m/s, the Charnock parameter is equal to 0.03, which is in agreement with the earlier data [71]. The measurements confirm the predominance of the viscous mechanism of roughness formation at winds <4 m/s, when the calculation by formula (21) is incorrect, and the effects of viscosity are to be taken into account. The wide spread of the experimental data on the roughness parameter at gentle winds can be due to the stratification, nonstationary wind field, the effect of direction, and low speed of wind [54].

Figure 2 compares the parameters of dynamic roughness, obtained by formulas (9), (25) (c = 0.11, a = 0.03), and (24) (m = 25). At medium wind speeds, the calculations by Charnock formula coincide with observation results. The overestimates by (24) are likely due to the fact that the parameterization was carried out for coastal regions with transformation of waves coming from the open sea. The values of the roughness parameter in the absence of wind $z_0 = 0.001$ m correspond to the data of model calculations for free convection regime in [37]. Overall, the parameter of dynamic roughness varies from 0.00007 to 0.0009 m.

The parameters of roughness for the momentum, heat, and moisture at medium winds averaged 0.0006, 0.000073, and 0.000069 m, respectively. Figure 3a shows the dependence of roughness parameters for the temperature and momentum on wind speed. Note that at weak wind, the roughness parameters for the temperature and humidity are not equal (Fig. 3b). The ratio of the roughness scales for temperature and moisture are far greater than unit for a weak wind and decrease to values near unit for wind above the threshold value ~3.0 m/s. The more efficient transfer of sensible heat than latent heat at weak winds $z_{0H} > z_{oT}$ is due to the fact that thermal flow plays a considerable role in the formation of the buoyancy flux.

The parameterizations obtained by the authors of this study from measurements are as follows:

$$z_{0u} = \max\left(0.03\frac{u_*^2}{g}, \frac{0.135\nu}{u_*}\right), \quad (34)$$

$$z_{ot} = z_0 \left\{-0.56(4\sqrt{\mathrm{Re}} - 3.4\right\}, \quad (35)$$

$$z_{oh} = z_0 \left\{-0.6(4\sqrt{\mathrm{Re}} - 3.6\right\}. \quad (36)$$

The coefficients in formulas (34)–(36) are close to the coefficients obtained before [62], thus demonstrating the manifestation of a single mechanism of transport processes in the viscous sublayer of closed water bodies.

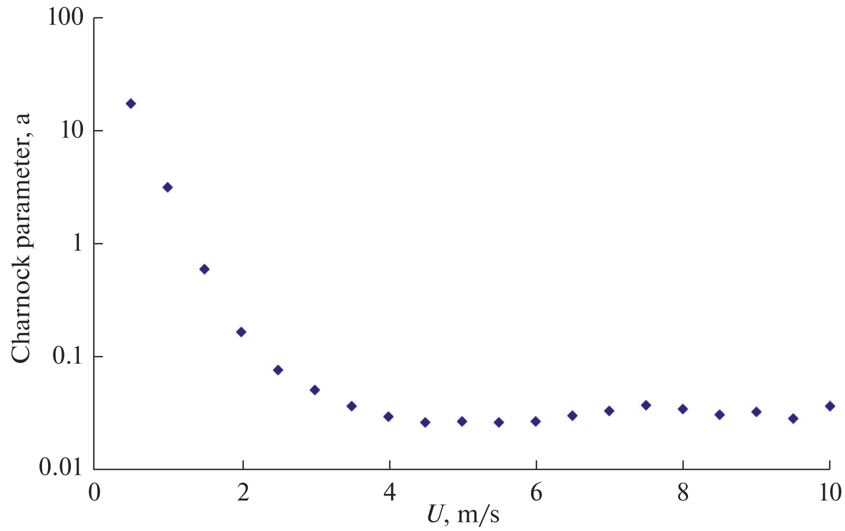

Fig. 1. Dependence of Charnock parameter (21), obtained from measurements in shallow-water areas, on wind speed U.

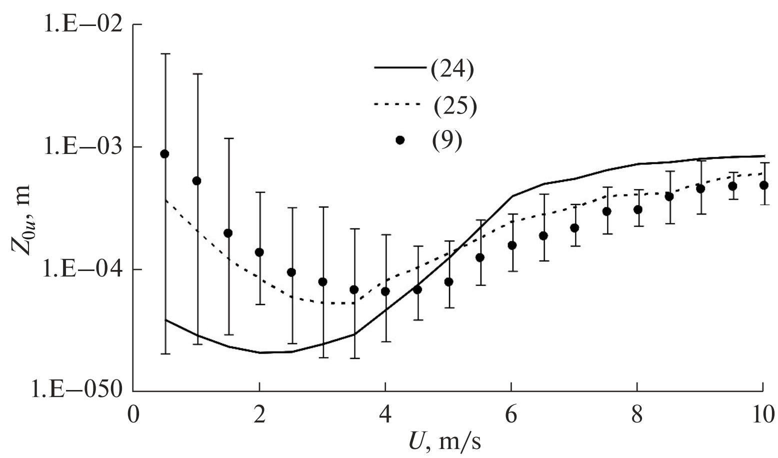

Fig. 2. Dynamic roughness parameter, determined by (9), (24), and (25), depending on wind speed U.

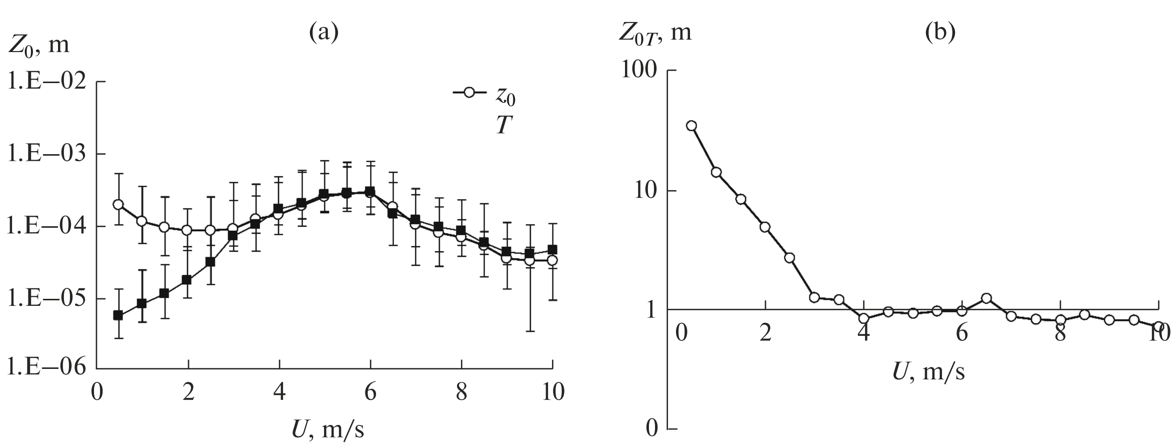

Fig. 3. (a) Dependence of roughness parameters for temperature and humidity, determined by formulas (10) and (11), on wind speed, (b) the ratio of the roughness parameter for temperature to the roughness parameter for humidity as a function of wind speed U.

CONCLUSIONS

This study of the roughness parameters of shallow water bodies uses the data of pulsation observations in different water areas. The results show that Charnock formula can be used to calculate the parameter of dynamic roughness for shallow closed water bodies. At medium wind speeds, the results of calculations by Charnock formula coincide with observation results; in this case, the Charnock parameter is three times as high as that for the open ocean. At weak winds, the roughness forms by the surface tension or small-scale capillary waves, and the Charnock relationship in the form (21) is inapplicable, because the effect of gravity winds decreases. In this case, the passage from a viscous mechanism to a wave mechanism takes place at wind speed higher than that in the ocean. At medium winds in the lake, the dynamic roughness is greater than in the open ocean. This is likely due to the fact that waves in the lake do not reach a large age and inherit the parameters of young waves under stronger wind.

The roughness parameters for the temperature and humidity at wind speed <3 m/s are not equal. The more efficient transport of sensible heat than latent heat at weak winds is due to the fact that thermal flow plays an important part in the formation of buoyancy flux. The numerical coefficients in the dependencies of the ratio of dynamic roughness to the roughness parameter for the temperature (humidity) on the Reynolds number are close to the values obtained before for other closed water bodies, thus demonstrating that the formation mechanism of the transport processes in the viscous sublayer is the same. The obtained parameterizations can be used in climate and lake models to calculate turbulent fluxes over continental water bodies.

FUNDING

This study was supported by the Russian Science Foundation, project nos. 21-17-00249, Processing and Analysis of Experimental Data, and 18-77-10066, Experimental Studies in the Gorky Reservoir; RF Ministry of Science within the framework of the Program of the Moscow Center for Fundamental and Applied Mathematics, agreement 075-15-2022-284, Development of Parameterizations, and partly under Governmental Order to the Water Problems Institute, Russian Academy of Sciences, subject FMWZ-2022-0001, Experimental Studies.

REFERENCES

1. Zilitinkevich, S.S., *Dinamika pogranichnogo sloya atmosfery* (Dynamics of the Atmospheric Boundary Layer), Monin, A.S, Ed., Leningrad: Gidrometeoizdat, 1970.
2. Krivitskii, S.V. and Stekalov, S.S., On the surface roughness parameter of shallow water bodies, *Izv. Akad. Nauk SSSR, Fiz. Atmosf. Okeana*, 1988, vol. 24, no. 1, pp. 103–106.
3. Mol'kov, A.A., Kapustin, I.A., Ermakov, S.A., Sergievskaya, I.A., Shomina, O.V., Lazareva, T.N., and Leshchev, G.V., Hydrophysical laboratory of IAPh RAS Geofizik as an efficient instrument of limnological monitoring, *Nauchnye problemy ozdorovleniya rossiiskikh rek i puti ikh resheniya* (Scientific Problems of the Restoration of Russian Rivers and Ways to Their Solution), 2019, pp. 214–218.
4. Monin, A.S. and Obukhov, A.M., Main regularities of turbulent mixing in the surface atmospheric layer, *Tr. Geofiz. Inst. AN SSSR*, 1954, no. 24, vol. 151, pp. 163–187.
5. Repina, I.A., Studying the dynamic characteristics and the regime of surface water temperature in the Caspian Sea, *Meteorol. Gidrol.*, 2000, no. 10, pp. 15–27.
6. Stepanenko, V.M., Repina, I.A., Fedosov, V.E., Zilitinkevich, S.S., and Lykosov, V.N., An overview of parameterezations of heat transfer over moss-covered surfaces in the Earth system models, *Izv., Atmos. Ocean. Phys.*, 2020, vol. 56, no. 2, pp. 101–111.
7. Anctil, F. and Donelan, M., Air-water momentum flux observations over shoaling waves, *J. Phys. Oceanogr.*, 1996, vol. 26, pp. 1344–1354.
8. Andreas, E.L. and Emanuel, K.A., Effects of sea spray on tropical cyclone intensity, *J. Atmos Sci.*, 2001, vol. 58, no. 24. vol. 3741–3751.
9. Andreas, E.L., Horst, T.W., Grachev, A.A., Persson, P.O.G., Fairall, C.W., Guest, P.S., and Jordan, R.E., Parametrizing turbulent exchange over summer sea ice and the marginal ice zone *Quarterly J. Royal Meteorol. Soc.*, 2010, vol. 136, no. 649, pp. 927–943.
10. Andreas, E.L., Jordan, R.E., and Makshtas, A.P., Parameterizing turbulent exchange over sea ice: the ice station Weddell results, *Bound. Layer Meteorol.*, 2005, vol. 114, no. 2, pp. 439–460.
11. Andreas, E.L., Persson, P.O.G., Grachev, A.A., Jordan, R.E., Horst, T.W., Guest, P.S., and Fairall, C.W., Parameterizing turbulent exchange over sea ice in winter, *J. Hydrometeorol.*, 2010, vol. 11, no. 1, pp. 87–104.
12. Artamonov, A.Yu., Buchnev, I.A., Repina, I.A., Skirta, A.Yu., Smirniov, A.S., and Tolpygin, L.I., Turbulent fluxes of heat and momentum and statistical characteristics of turbulence in the near-surface air in near-shore and deep-water zones of the Black Sea, *Oceanology*, 2005, vol. 45. Suppl. 1, pp. S27–S38.
13. Ataktürk, S.S. and Katsaros, K.B., Wind stress and surface waves observed on Lake Washington, *J. Phys. Oceanogr.*, 1999, vol. 29, no. 4, pp. 633–650.
14. Brutsaert, W., *Evaporation into the Atmosphere: Theory, History and Applications*, Dordrecht: Springer Sci. Business Media, 2013.
15. Burba, G., *Eddy Covariance Method for Scientific, Industrial, Agricultural and Regulatory Applications: A Field Book on Measuring Ecosystem Gas Exchange and Areal Emission Rates*, Lincoln: LI-COR Biosci., 2013.

16. Businger, J.A., Wyngaard, J.C., and Bradley, E.F. Flux profile relationships in the atmospheric surface layer, *J. Atmos. Sci.*, 1971, vol. 28, pp. 181–189.

17. Charnock, H., A note on empirical wind-wave formulae, *Quarterly J. Royal Meteorol. Soc.*, 1958, vol. 84, pp. 443–447.

18. Charnock, H. Wind stress on water surface, *Quarterly J. Royal Meteorol. Soc.*, 1955, vol. 81, pp. 639–640.

19. Diallo, I., Giorgi, F., and Stordal, F., Influence of Lake Malawi on regional climate from a double-nested regional climate model experiment, *Clim. Dynam.*, 2018, vol. 50, nos. 9–10, pp. 3397–3411.

20. Dias, N.L. and Vissotto, D., The effect of temperature–humidity similarity on Bowen ratios, dimensionless standard deviations, and mass transfer coefficients over a lake, *Hydrol. Process.*, 2017, vol. 31, pp. 256–269.

21. Donelan, M.A., Haus, B.K., Reul, N., Plant, W.J., Stiassnie, M., Graber, H.C., Brown, O.B., and Saltzman, E.S., On the limiting aerodynamic roughness of the ocean in very strong winds, *Geophys. Res. Lett.*, 2004, vol. 31, L18306.

22. Drennan, W.M., Graber, H.C., Hauser, D., and Quentin, C., On the wave age dependence of wind stress over pure wind seas, *J. Geophys. Res.*, 2003, vol. 108, pp. 8062.

23. Dyer, A.J., A review of flux-profile relationships, *Boundary-Layer Meteorol.*, 1974, vol. 7, pp. 363–372.

24. Fairall, C.W., Bradley, E.F., Hare, J.E., Grachev, A.A., and Edson, J.B., Bulk parameterization of air–sea fluxes: updates and verification for the COARE algorithm, *J. Climate*, 2003, vol. 16, no. 4, pp. 571–591.

25. Fairall, C.W., Bradley, E.F., Rogers, D.P., Edson, J.B., and Young, G.S., Bulk parameterization of air-sea fluxes for tropical ocean-global atmosphere coupled-ocean atmosphere response experiment, *J. Geophys. Res.: Oceans*, 1996, vol. 101 (C2), pp. 3747–3764.

26. Fisher, A.W., Sanford, L.P., and Suttles, S.E., Wind stress dynamics in Chesapeake Bay: spatiotemporal variability and wave dependence in a fetch-limited environment, *J. Phys. Oceanogr.*, 2015, vol. 45, pp. 2679–2696.

27. Foken, T., 50 years of the Monin–Obukhov similarity theory, *Bound. Layer Meteorol.*, 2006, vol. 119, pp. 431–447.

28. Foken, T., Göockede, M., and Mauder, M., Post-field data quality control. Handbook of micrometeorology, *Handbook of Micrometeorology: A Guide for Surface Flux Measurement and Analysis*, X. Lee, W.J. Massman, and B. Law, Eds., Dordrecht: Kluwer Acad. Publ., 2004, pp. 181–208.

29. Garratt, J., Review of drag coefficients over oceans and continents, *Mon. Wea. Rev.*, 1977, vol. 105, pp. 915–929.

30. Garrat,t J.R., *The Atmospheric Boundary Layer*, Cambridge UK: Cambridge Univ. Press, 1997.

31. Gerken, T., Biermann, T., Babel, W., Herzog, M., Ma, Y., Foken, T., and Graf, H.-F., A modelling investigation into lake-breeze development and convection triggering in the Nam Co Lake basin, Tibetan Plateau, *Theor. Appl. Climatol.*, 2014, vol. 117, nos. 1–2, pp. 149–167.

32. Grachev, A.A., Bariteau, L., Fairall, C.W., Hare, J.E., Helmig, D., Hueber, J., and ang, E.K., Turbulent fluxes and transfer of trace gases from shipbased measurements during TexAQS 2006, *J. Geophys. Res.*, 2011, vol. 116, p. D13110.

33. Grachev, A.A., Fairall, C.W., and Larsen, S.E., On the determination of the neutral drag coefficient in the convective boundary layer, *Boundary-Layer Meteorol.*, 1998, vol. 86, pp. 257–278.

34. Heikinheimo, M., Kangas, M., Tourula, T., Venäläinen, A., and Tattari, S., Momentum and heat fluxes over lakes Tämnaren and Råksjö determined by the bulk-aerodynamic and eddy-correlation methods, *Agr. Forest Meteorol.*, 1999, v. 98, pp. 521–534.

35. Hicks, B.B. Some evaluations of drag and bulk transfer coefficients over water bodies of different sizes, *Bound. Layer Meteorol.*, 1972, vol. 3, no. 2, pp. 201–213.

36. Högström, U., Non-dimensional wind and temperature profiles in the atmospheric surface layer: a re-evaluation, *Bound. Layer Meteorol.*, 1988, vol. 42, pp. 55–78.

37. Huang, C.H., Modification of the Charnock wind stress formula to include the effects of free convection and swell, *Advanced Methods for Practical Applications in Fluid Mechanism*, Steven, J., Ed., London: InTech, 2012, pp. 47–69.

38. Istvánovics, V., and Honti, M., Coupled simulation of high frequency dynamics of dissolved oxygen and chlorophyll widens the scope of lake metabolism studies, *Limnol. Oceanogr.*, 2018, vol. 63, pp. 72–90.

39. Johnson, H.K., Højstrup, J., Vested, H.J., and Larsen, S.E., On the dependence of sea surface roughness on wind waves, *J. Phys. Oceanogr.*, 1998, vol. 28, pp. 1702–1716.

40. Kitaigorodskii, S.S., Volkov, Yu.A., and Grachev, A.A., A note on the analogy between momentum transfer across a rough solid surface and the air-sea interface, *Boundary-Layer Meteorol.*, 1995, vol. 74, pp. 1–17.

41. Kormann, R. and Meixner, F.X., An analytical footprint model for non-neutral stratification, *Boundary-Layer Meteorol.*, 2001, vol. 99, no. 2, pp. 207–224.

42. Langleben, M.P., A study of the roughness parameters of sea ice from wind profiles, *J. Geophys. Res.*, 1972, vol. 77, no. 30, pp. 5935–5944.

43. Li, D., Rigden, A., Salvucci, G., and Liu, H., Reconciling the Reynolds number dependence of scalar roughness length and laminar resistance, *Geophys. Res. Lett.*, 2017, vol. 44, no. 7, pp. 3193–3200.

44. Li, Z., Lyu, S., Zhao, L., Wen, L., Ao, Y., and Wang, S., Turbulent transfer coefficient and roughness length in a high-altitude lake, Tibetan Plateau, *Theor. Applied Climatol.*, 2016, vol. 124, no. 3, pp. 723–735.

45. Liu, W.T., Katsaros, K.B., and Businger, J.A., Bulk parameterization of air-sea exchange of heat and water vapor including the molecular constraints at the interface, *J. Atmos. Sci.*, 1979, vol. 36, pp. 1722–1735.

46. Long, Z., Perrie, W., Gyakum, J., Caya, D., and Laprise, R., Northern lake impacts on local seasonal climate, *J. Hydrometeorol.*, 2007, vol. 8, no. 4. pp. 881–896.

47. Mahrt, L., Vickers, D., Frederickson, P., Davidson, K., and Smedman, A.S., Sea-surface aerodynamic roughness, *J. Geophys. Res.*, 2003, vol. 108, (C6), p. 3171.

48. Mahrt, L., Vickers, D., Sun, J., Jensen, N.O., Jørgensen, H., Pardyjak, E., and Fernando, H., Determination of the surface drag coefficient, *Bound. Layer Meteorol.*, 2000, vol. 99, no. 2, pp. 249–276.

49. Moat, B.I., Yelland, M.J., and Pascal, R.W., Quantifying the airflow distortion over merchant ships. Part 1: Validation of a CFD model, *J. Atmos. Oceanic Technol.*, 2006, vol. 23, pp. 341–350.

50. Moncrieff, J.B., Clement, R., Finnigan, J., and Meyers, T., Averaging detrending and filtering of eddy covariance time series, *Handbook of Micrometeorology: A Guide for Surface Flux Measurements*, Lee, X., Massman, W.J., Law, B.E., Eds., Dordrecht: Kluwer Acad., 2004. pp. 7–31.

51. Olabarrieta, M., Warner, J.C., Armstrong, B., Zambon, J.B., and He, R., Ocean-atmosphere dynamics during Hurricane Ida and Nor'Ida: An application of the coupled ocean–atmosphere–wave sediment transport (COAWST) modeling system, *Ocean Model.*, 2012, vol. 43–44, pp. 112–137.

52. Panin, G.N., Nasonov, A.E., Foken, T., and Lohse, H., On the parameterization of evaporation and sensible heat exchange for shallow lakes, *Theor. Appl. Climatol.*, 2006, P. 85 (3–4), pp. 123–129.

53. Paulson, C.A., The mathematical representation of wind speed and temperature profiles in the unstable atmospheric surface layer, *J. Appl. Meteorol.*, 1970, vol. 9, pp. 857–861.

54. Repina, I., Artamonov, A., Chukharev, A., Esau, I., Goryachkin, Y., Kuzmin, A., Pospelov, M., Sadovsky, I., and Smirnov, M., Air–sea interaction under low and moderate winds in the Black Sea coastal, *Estonian J. Engineering*, 2012, vol. 18, no 2, pp. 89–101.

55. Shabani, B., Nielsen, P., and Baldock, T., Direct measurements of wind stress over the surf zone, *J. Geophys. Res.*, 2014, vol. 119, pp. 2949–2973.

56. Sharma, A., Hamlet, A.F., Fernando, H.J.S., Catlett, C.E., Horton, D.E., Kotamarthi, V.R., et al., The need for an integrated land–lake–atmosphere modeling system, exemplified by North America's Great Lakes region, *Earth's Future*, 2018, vol. 6, pp. 1366–1379.

57. Smith, S., Coefficients for sea surface wind stress, heat flux, and wind profiles as a function of wind speed and temperature, *J. Geophys. Res-Oceans*, 1988, vol. 93 (C12), pp. 15467–15472.

58. Smith, S.D., Anderson, R.J., Oost, W.A., Kraan, C., Maat, N., De Cosmo, J., Katsaros, K.B., Davidson, K.L., Bumke, K., Hasse, L., and Chadwick, H.M., Wind stress and drag coefficients, *Bound.-Lay. Meteorol.*, 1992, vol. 60, pp. 109–142.

59. Solheid, B., Dias, N., Armani, F., and Junior, D.V., Evaluation of alternatives for parameterization of momentum and water vapor roughness lengths in lakes, *Revista Internacional de Métodos Numéricos para Cálculo y Diseño en Ingeniería*, 2020, vol. 36, no. 2, pp. 1–11.

60. Soloviev, A. and Lukas, R., The near-surface layer of the ocean: structure, dynamics and applications, *Springer Sci. Business Media*, 2013, vol. 48, p. 551.

61. Stepanenko, V.M., Repina, I.A., Artamonov, A.Y., Gorin, S.L., Lykossov, V.N., and Kulyamin, D.V., Mid-depth temperature maximum in an estuarine lake, *Environ. Res. Lett.*, 2018, vol. 13, no. 3, p. 035006.

62. Subin, Z.M., Riley, W.J., and Mironov, D., An improved lake model for climate simulations: model structure, evaluation, and sensitivity analyses in CESM1, *J. Adv. Model Earth Syst.*, 2012, vol. 4, p. M02001.

63. Toba, Y. and Koga, M., A parameter describing overall conditions of wave breaking, whitecapping, sea-spray production and wind stress, *Oceanic Whitecaps*, Y. Toba, Ed., Amsterdam: Springer Netherlands, 1986, pp. 37–47.

64. Torma, P. and Krámer, T., Modeling the effect of waves on the diurnal temperature stratification of a shallow lake, *Period. Polytech. Civ. Eng.*, 2017, vol. 61, pp. 165–175.

65. Van Dijk, A., Moene, A.F., and de Bruin, H.A.R., *The Principles of Surface Flux Physics: Theory, Practice and Description of the ECPack Library*, Wageningen: Wageningen Univ., 2004.

66. Varentsov, A.I., Zilitinkevich, S.S., Stepanenko, V.M., Tyuryakov, S.A., and Alekseychik, P.K., Thermal roughness of the fen surface, *Boundary-Layer Meteorol.*, 2022, pp. 1–15.

67. Verburg, P. and Antenucci, J.P., Persistent unstable atmospheric boundary layer enhances sensible and latent heat loss in a tropical great lake: Lake Tanganyika, *J. Geophys. Res.*, 2010, vol. 115 (D11), pp. D11109.

68. Vickers, D. and Mahrt, L., Sea-surface roughness lengths in the midlatitude coastal zone, *Quarterly J. Royal Meteorol. Soc.*, 2010, vol. 136, no. 649, pp. 1089–1093.

69. Vickers, D. and Mahrt, L., Quality control and flux sampling problems for tower and aircraft data, *J. Atmos. Ocean. Technol.*, 1997, vol. 14, pp. 512–526.

70. Wang, B. and Ma, Y., On the simulation of sensible heat flux over the Tibetan Plateau using different thermal roughness length parameterization schemes, *Theor. Applied Climatol.*, 2019, vol. 137, no. 3, pp. 1883–1893.

71. Wang, B., Ma, Y., Chen, X., Ma, W., Su, Z., and Menenti, M., Observation and simulation of lake-air heat and water transfer processes in a high-altitude shallow lake on the Tibetan Plateau, *J. Geophys. Res.: Atmosph.*, 2015, vol. 120, no. 24, pp. 12327–12344.

72. Wang, B., Ma, Y., Wang, Y., Su, Z., and Ma, W., Significant differences exist in lake-atmosphere interactions and the evaporation rates of high-elevation small and large lakes, *J. Hydrol.*, 2019, vol. 573, pp. 220–234.

73. Webb, E.K., Pearman, G.I., and Leuning, R., Correction of flux measurements for density effects due to heat and water vapour transfer, *Quarterly J. Royal Soc.*, 1980, vol. 106, pp. 85–100.

74. Webster, P.J. and Lukas, R., TOGA COARE: The Coupled Ocean—Atmosphere Response Experiment, *Bull. Am. Meteorol. Soc.*, 1992, vol. 73, no. 9, vol. 1377–1416.
75. Wu, J., The sea surface is aerodynamically rough even under light winds, *Bound.-Layer Meteorol.*, 1994, vol. 69, nos. 1–2, pp. 149–158.
76. Wu, J., Wind-stress coefficients over sea surface near neutral conditions—a revisit, *J. Phys. Oceanogr.*, 1980, vol. 10, pp. 727–740.
77. Wüest, A. and Lorke, A., Small scale hydrodynamics in lakes, *Annu. Rev. Fluid. Mech.*, 2003, vol. 35, pp. 373–412.
78. Yang, K., Koike, T., Ishikawa, H., Kim, J., Li, X., Liu, H., and Wang, J., Turbulent flux transfer over bare-soil surfaces: characteristics and parameterization, *J. Appl. Met. Clim.*, 2008, vol. 47, no. 1, pp. 276–290.
79. Zilitinkevich, S., Grachev, A., and Fairall, C., Scaling reasoning and field data on the sea-surface roughness lengths for scalars, *J. Atmos. Sci.*, 2001, vol. 58, pp. 320–325.
80. Zilitinkevich, S.S., Mammarella, I., Baklanov, A.A., and Joffre, S.M., The effect of stratification on the roughness length and displacement height, *Boundary-Layer Meteorol.*, 2008, vol. 129, pp. 179–190.